Electronic Supplementary Material (ESI) for Journal of Materials Chemistry B.

Light–driven assembly of biocompatible fluorescent chitosan hydrogels with self–healing ability

Olatz Guaresti[1], Leander Crocker[2], Teodoro Palomares[3], Ana Alonso–Varona[3], Arantxa Eceiza[1], Ljiljana Fruk[2], Nagore Gabilondo[1,*]

[1]'Materials + Technologies' Group, Department of Chemical and Environmental Engineering, Engineering College of Gipuzkoa, University of the Basque Country, Plaza Europa 1, 20018 Donostia- San Sebastián, Spain

[2]BioNano Engineering Group, Department of Chemical Engineering and Biotechnology, University of Cambridge, West Cambridge Site, Philippa Fawcett Drive CB3 0AS, Cambridge, UK

[3]Department of Cell Biology and Histology, Faculty of Medicine and Dentistry, University of the Basque Country, Barrio Sarriena s/n, 48940 Leioa, Spain

SUPPLEMENTARY INFORMATION

EXPERIMENTAL SECTION

Materials. The following chemicals were used as received: chitosan (Cs, Sigma–Aldrich), β–alanine (99 %, Sigma–Aldrich), maleic anhydride (98 %, Panreac), N–hydroxysuccinimide (NHS, 98 %, Sigma–Aldrich), 1–ethyl–3–(3–dimethylaminopropyl carbodiimide hydrochloride) (EDC, purum ≥ 98%, Sigma–Aldrich), 4–formylbenzoic acid (98 %, Alfa), ρ–toluenesulfonyl hydrazide (98 %, Alfa), ρ–Anisidine (≥ 99 %, Sigma–Aldrich), sodium nitrite ($NaNO_2$, 98 %, Merck), pyridine (99.5 %, Acros), glacial acetic acid solution (HAc, for analysis, 99.8 %, Panreac), hydrochloric acid solution (HCl, for analysis, 37 %, Panreac), ethanol (EtOH, for analysis, 96 %, Panreac), methanol (for HPLC, ≥ 99.9 %, Sigma–Aldrich), acetone (Oppac S.A.), phosphate buffered saline tablets (PBS, pH = 7.4, PanReac), anhydrous N,N–dimethylformamide (DMF, Acros) and dimethyl sulfoxide (DMSO, VWR). Deuterium oxide (deuteration degree 99.96 %, Merck) was used for ^{1}H NMR analysis and deionized water was employed as solvent.

The average molecular weight (M_W) of the sample was estimated by a general viscometry method using an automated capillary viscometer at 25 ºC and it was found to be of 67 kDa (low molecular weight range). Besides, the degree of acetylation (DAc) of the chitosan was calculated from the ^{1}H NMR spectrum and then, the degree of deacetylation (DDc) was determined as the difference with DAc following the same procedure of our previous work,[1] being 80 %.

Methods. Liquid–state ^{1}H NMR measurements were conducted with an Avance Bruker 500 spectrometer equipped with a BBO probe with gradient in Z axis, at a frequency of 500 MHz, number of scans 64, spectral window of 5000 Hz and recovery delay of 1 s. A mixture of D_2O/HCl (0.5 M) in 1:10 (v/v) ratio at 80 ºC was employed as solvent.

The degree of substitution (DS) of maleimide–functionalized chitosan was calculated from the area (A) of the proton signal corresponding to the maleimide ring and those of the glucosamine repeating unit from the carbons that were not affected by the functionalization (3 to 6), with a 5/2 ratio between them, respectively (Equation S1).

$$DS_{CsMal}(\%) = \left(\frac{5 \cdot A_{Mal}}{2 \cdot A_{Cs}} \right) \cdot 100 \qquad \text{(S1)}$$

Solid–state ^{13}C NMR spectra were recorded on a Bruker AVANCE III, 9.4 T equipped with a MASDVT BL4 X//H Probe head at a spinning rate of 10 kHz. ^{13}C chemical shifts were calibrated indirectly with glycine. The spectra were recorded with a delay between scans of 15 s and the number of scans were 10240.

For the tetrazole–functionalized chitosan the degree of substitution was determined by the integration of the areas of the carbon signals of the glucosamine units and those of the tetrazole unit that were not affected (3 to 5), with a 3/11 ratio between them. Calculations were made using Equation S2.

$$DS_{CsTZ}(\%) = \left(\frac{3 \cdot A_{TZ}}{11 \cdot A_{Cs}} \right) \cdot 100 \qquad \text{(S2)}$$

The XRD patterns were measured using PHILIPS X´Pert Pro automatic diffractometer, in theta–theta configuration secondary monochromator with Cu Kα radiation (λ = 0.154 nm) and a PIXcel solid state detector (active length in 2θ = 3.347º), operating at 40 kV with a filament of 40 mA. The diffractograms were collected in the region 2θ = 5 to 80º, where θ is the angle of incidence of the X–ray beam on the sample. The crystallinity index (CI^{XRD}) was calculated using Equation S3.

$$CI^{XRD} = \frac{I_{110} - I_{am}}{I_{110}} \qquad \text{(S3)}$$

where I_{110} is the maximum intensity (arbitrary units) of the (110) diffraction peak at 2θ = 20º and I_{am} is the intensity of the amorphous diffraction signal at 2θ = 16º. [2–5]

Fluorescence emission spectra were recorded on a Cary Eclipse Fluorescence Spectrophotometer (Agilent Technologies) at an excitation wavelength of 396 nm. The influence of the irradiation time (after 1 and 2 hours of reaction) and the solvent (HCl (pH 1) and PBS (pH 7.4)) on the fluorescent properties of the tetrazole/maleimide hydrogels was studied. Thin dried samples were placed in a micro quartz cuvette of 200 µL in a 45º angle, which was placed in the sample

holder. The spectra were recorded from 380 nm to 700 nm at an excitation slit width of 5 nm, an emission slit width of 5 nm, a resolution of 1 nm and a scan rate of 600 nm min^{-1}.

The insoluble fraction of the cross–linked materials was estimated as the gel fraction (Gel). The hydrogels were immersed in PBS at 37 ºC for 3 h, based on equilibrium swelling time studies. The gel fraction of the hydrogels was determined by Equation S4.

$$\text{Gel}\ (\%) = \frac{W_t}{W_0} \cdot 100 \qquad \text{(S4)}$$

where W_0 and W_t are the initial and final weights of the hydrogel sample referred to the dry state.

The dynamic rheological behaviour of the synthesized hydrogels was studied by frequency sweep tests. Thereby, the storage modulus (G´), loss modulus (G´´) and the damping factor (tan δ) of the final hydrogels were calculated by oscillatory rheometry using a Rheometric Scientific Advanced Rheometric Expansion System (ARES) and parallel plate geometry (diameter 25 mm) as described, in oscillation mode at 37 ºC. After the determination of the linear viscoelastic region (LVR) from stress sweep study, frequency sweep analyses were evaluated from 0.1 to 500 rad s^{-1} at a fixed strain of 1 %. The damping factor describes the ratio between the two portions of the viscoelastic behaviour (G´ and G´´), i.e. for ideally elastic behaviour tan δ = 0 whereas tan δ = 1 for ideally viscous behaviour.

Based on the rheological results, the structural parameters of the developed hydrogels were determined. The average mesh size (ξ, nm), the cross–linking density (n_e, mol m^{-3}) and the average molecular weight between neighbouring

cross–links (M_c, kg mol^{-1}), were calculated based on the so–called rubber elastic theory (RET) from Equation S5, S6 and S7, respectively.[6]

$$\xi = \left(\frac{G' \cdot N_A}{RT} \right)^{-1/3} \quad \text{(S5)}$$

$$n_e = \frac{G_e}{RT} \quad \text{(S6)}$$

$$M_c = \frac{c\rho RT}{G_e} \quad \text{(S7)}$$

where G´ is the storage modulus, N_A is the Avogadro constant ($6.022 \cdot 10^{23}$), R is the gas constant (8.314 J K^{-1} mol^{-1}), T is the temperature (310 K), G_e represents the plateau value of storage modulus measured by frequency sweep test (being equal to the value of G´ for covalently cross–linked hydrogels), c is the polymer concentration in the hydrogels (18 and 6 % w/v for CsTZ/CsMal_1 and CsTZ/CsMal_2, respectively) and ρ is the density of water at 310 K (993 kg m^{-3}).

The shear–thinning and the yield point were analysed in a Haake Viscotester IQ Thermo Scientific using the parallel plate geometry (titanium upper plate of 35 mm and steel lower plate of 60 mm) at room temperature. To measure the shear–thinning property, the viscosity of the hydrogels was studied under steady shear strain measurements in the range of 0.1 to 1000 s^{-1} in rotatory mode. Besides, oscillatory stress sweep experiments were carried out in order to estimate the yield point. Below the critical stress amplitude (LVR), the material responds as a solid (G´ > G´´) and G´ and G´´ are independent of the applied stress. At higher stress values, G´ decreases and G´ and G´´ cross.

From this point onwards, the viscous character of the material will dominate.[7] The yield point was studied by recording the evolution of storage and loss moduli at a given frequency of 1 Hz in a shear stress (τ) range from 1 to 1000 Pa. The crossover point will determine the yield point.

The self–healing ability measurements were conducted in a Haake Viscotester IQ Thermo Scientific using the parallel plate geometry and was assessed by registering the variation of the storage and loss moduli in step–strain measurements at a fixed frequency of 1 Hz at room temperature. Samples were treated for 60 seconds under very low strain (0.1 %), which is substantially under the deformation limit. Subsequently, the strain was increased above the critical region (50 %) for 60 seconds and afterwards, the cycle was completed by descending again the applied strain (0.1 %).

The healing efficiency of the NITEC hydrogels was determined by the relationship between the modulus values at 0.1 % strain, both storage (G´) and (G´´) loss moduli, before (a) and after (b) subjecting to 50 % strain by applying the Equations S8 and S9.

$$\text{Healing efficiency}_{G'}\ (\%) = \frac{G'_{0.1\ (b)}}{G'_{0.1\ (a)}} \cdot 100 \qquad \text{(S8)}$$

$$\text{Healing efficiency}_{G''}\ (\%) = \frac{G''_{0.1\ (b)}}{G''_{0.1\ (a)}} \cdot 100 \qquad \text{(S9)}$$

All the rheological tests were conducted in triplicate.

Scanning electron microscopy (SEM) images were performed by a JEOL JSM–6400 with a wolframium filament operating at an accelerated voltage of 20 kV

and at a working distance of 15 mm. Prior to SEM assay, samples were fractured in order to expose the cross–section and coated with approximately 20 nm of chromium using a Quorum Q150 TES metallizer.

The swelling capacity of freeze–dried hydrogels was studied by a general gravimetric method. Samples were immersed in different medium, PBS (pH 7.4) and 0.1 M HCl (pH 1), simulating intestinal and gastric fluids, respectively) at 37 ºC. At selected time intervals after immersion (1/4, 1/2, 1, 2 and 24 or 48 h), the swollen samples were removed, weighed once the excess of liquid was withdrawn with filter paper and again freeze–dried. The equilibrium swelling was considered to be achieved when the weight of the hydrogels no longer increased. The swelling ratio (SR) was calculated using the following Equation S10.

$$SR\ \ (\%) = \left(\frac{W_S - W_d}{W_d} \right) \cdot 100 \qquad \text{(S10)}$$

where W_s and W_d are the weight of the swollen and final freeze–dried hydrogel samples, respectively. The assay was conducted in triplicate.

The swelling kinetics of the hydrogels was adjusted following a previously reported method for this type of materials, which is based on Equation S11.[8]

$$\frac{t}{SR} = \frac{1}{SR_{max}^2 \cdot k_s} + \frac{1}{SR_{max}} \cdot t \qquad \text{(S11)}$$

where SR is the swelling ratio at time t, SR_{max} the maximum swelling value and k_S ($g_{hydrogel}\ g_{solution}^{-1}\ s^{-1}$) the swelling constant rate. The initial swelling rate (r_o, $g_{solution}\ g_{hydrogel}^{-1}\ s^{-1}$) was obtained from $1/(SR^2_{max} \cdot k_S) = 1/(dSR/dt)_0$. The swelling

process in all cases followed second order kinetics with correlation coefficients above 0.99.

In vitro degradation studies were carried out by gravimetric analysis according to a method described elsewhere. [8–11] Dried samples (4–10 mg) were weighed (W_0) and immersed in PBS for prescribed days at 37 ºC with 1 mg mL^{-1} lysozyme (≥ 40000 units mg^{-1} protein from chicken egg white). Samples were removed at fixed time intervals (2, 7, 14, 21 and 28 days) and washed out with deionized water to eliminate any superficial buffer and lysozyme traces. Samples were finally dried and weighed until constant value (W_t). Hydrolytic degradation was also studied as the control reference by incubation in lysozyme–free PBS solution at the same conditions. The measurements were performed in triplicate and the weight loss of the samples was calculated using Equation S12.

$$\text{Degradation } (\%) = \left(\frac{W_0 - W_t}{W_0} \right) \cdot 100 \qquad \text{(S12)}$$

where W_0 and W_t are the dried weights of the samples at initial and final time, respectively.

To assess *in vitro* cell response of the hydrogels, a short–term cytotoxicity assay was performed, in order to evaluate the presence and/or release of toxic degradation products, following ISO 10993 recommendations. Cytotoxicity was assessed by PrestoBlue® (Invitrogen, USA), a resazurin–based solution that functions as a colorimetric cell viability indicator. Briefly, murine fibroblasts (L929 cells) were seeded into 96–well plates at a density of $4 \cdot 10^3$ cells/well in 100 µL of complete standard culture medium (Dulbecco´s Modified Eagle´s

Medium, DMEM, Gibco, EEUU) that was supplemented with 10 % fetal bovine serum, 1 % of non essential aminoacids, 1 mM sodium pyruvate and 1 % penicillin/streptomycin. After 24 h, the medium was replaced with 100 µL of negative control (complete medium), positive control (complete medium/DMSO mix in 10:1 ratio) or sterilized hydrogel extractive media and a 10 % of PrestoBlue® was added. The optical density was measured at 570 nm in a spectrophotometer (Biotek, HT Synergy, USA) at different time points (0, 24 and 48 h). The viability of the cells was calculated following the Equation S13.

$$\text{Viability } (\%) = \frac{[\text{Abs}]_{\text{sample}}}{[\text{Abs}]_{\text{negative control}}} \cdot 100 \qquad \text{(S13)}$$

where $[Abs]_{sample}$ is the absorbance of the sample cells and $[Abs]_{negative\ control}$ is the absorbance of the negative control cells. All assays were conducted in triplicate and average values and standard deviations were estimated.

Synthesis of maleimide–functionalized chitosan (CsMal). Maleimide–functionalized chitosan (CsMal) was synthesized in aqueous environment according to the method described in our previous work[1]. Indeed, CsMal precursor was achieved by amide coupling conjunction with a maleimide–end acid (AMI) at an equivalent ratio of 1:2 for amine–to–carboxylic acid. Once the reaction of modification took place, the pH of the final product was maintained at 5 after the purification step via dialysis against deionized water for 72 h. Finally, CsMal was stored in solution ($3 \cdot 10^{-3}$ g mL^{-1}) at -28 ºC until needed for further use.

Synthesis of 4–(2–(4–methoxyphenyl)–2H–tetrazol–5–yl)benzoic acid (TBA). An acid precursor containing tetrazole groups was first synthesized

following a reported method in the literature[12] (Scheme S1) for later functionalization of chitosan. Thus, the desired molecule (4–(2–(4–methoxyphenyl)–2H–tetrazol–5–yl)benzoic acid, TBA) was obtained by two–step procedure. Namely, a mixture of 4–formylbenzoic acid (6.558 g, 43.7 mmol) and ρ–toluenesulfonyl hydrazide (8.138 g, 43.7 mmol) (A) in 100 mL of ethanol was heated to reflux for 30 min in a 1:1 equivalent ratio. The solution was diluted with 100 mL of water and the precipitate was filtered off. The solid (4–((2–tosylhydrazono)methyl)benzoic acid) was washed with 100 mL of aqueous ethanol (98 % w/w yield).

Subsequently, ρ–Anisidine (4 g, 32.5 mmol) was dissolved in a mixture of 8.46 mL of concentrated HCl, 26.9 mL of H_2O and 26.9 mL of EtOH and cooled to 0 ºC. A cooled solution of $NaNO_2$ (2.241 g, 32.5 mmol) in 13.45 mL of H_2O was added dropwise and stirred for 10 min at 0 ºC, being 1:1 the equivalent ratio of ρ–Anisidine to $NaNO_2$. The *in situ* generated diazonium salt solution (B) was added dropwise to a solution of (4–((2–tosylhydrazono)methyl)benzoic acid) (10.34 g, 32.5 mmol) in 200 mL of pyridine at 1:1 equivalent ratio at -10 ºC – -5 ºC over a period of 45 min. After complete addition, the solution was stirred at 0 ºC for 30 min and then, at ambient temperature overnight. The turbid solution was poured into 500 mL of 10 % v/v aqueous HCl solution and the precipitate (TBA) was filtered off and washed with 250 mL of EtOH (65 % w/w yield).

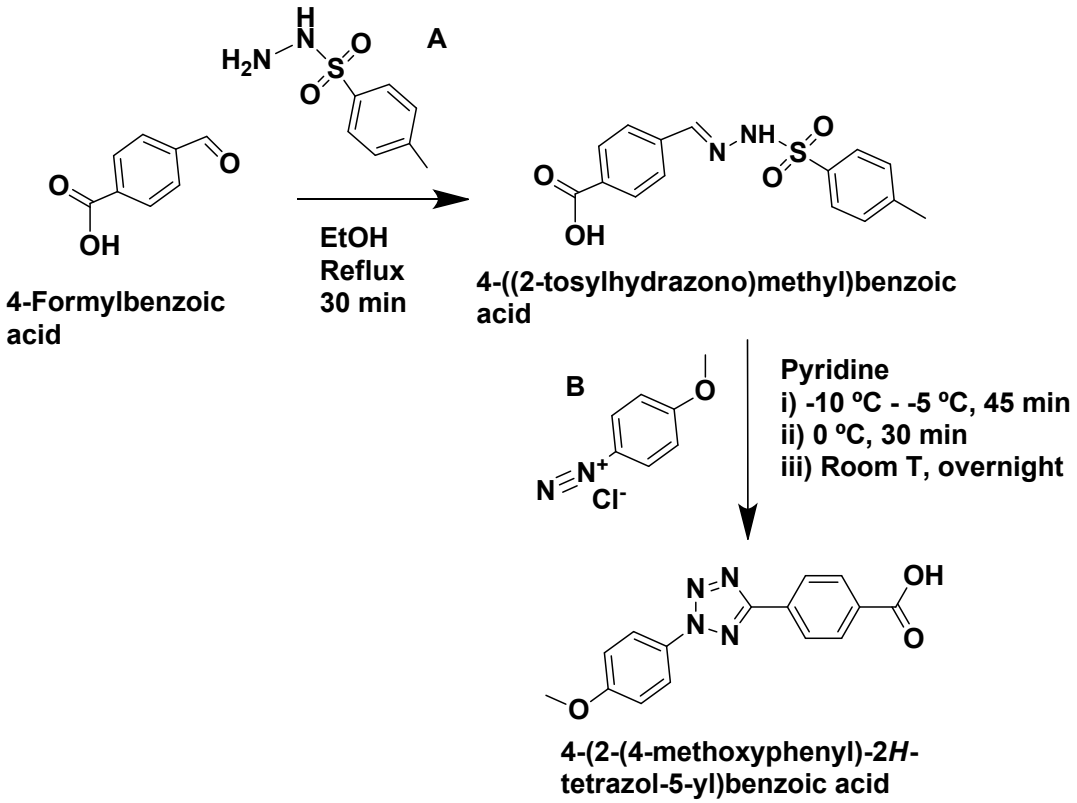

Scheme S1. Synthesis of 4–(2–(4–methoxyphenyl)–2*H*–tetrazol–5–yl)benzoic acid.

Synthesis of tetrazole–functionalized chitosan (CsTZ). The tetrazole–modified chitosan (CsTZ) was prepared via carbodiimide conjugation in DMF and under argon atmosphere. An equivalent ratio of 1:1.5 for amine–to–carboxylic acid was fixed in this case. Scheme S2 shows the reaction between TBA and chitosan. Firstly, 0.3 g of chitosan were dissolved in 1 % v/v aqueous acetic acid to a final concentration of 1 % w/v, while the pH of the solution was adjusted to 5–6 using 1 M NaOH. At the same time, TBA (0.066 g mL^{-1}) was activated in DMF for 1 hour with EDC and NHS in 1:1 and 1:1.1 molar ratios, respectively. The activated acid was added dropwise to the chitosan solution and the mixture was stirred overnight under magnetic stirring in dark at ambient temperature under argon atmosphere. The product was precipitated in acetone, washed with methanol and DMSO and centrifuged several times against deionized water (4200 rpm, 20 ºC and 15 min per cycle (x4)). Finally,

CsTZ was lyophilized (64 % w/w yield) and stored in dark at 4 ºC until further characterization.

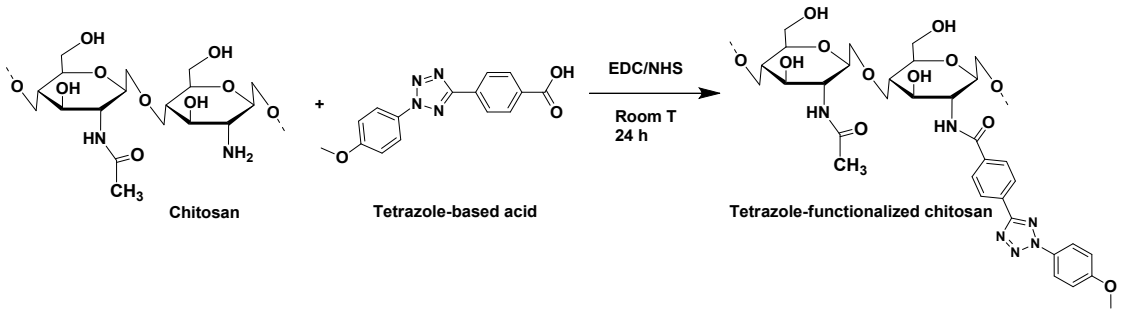

Scheme S2. Synthesis of CsTZ through the reaction of chitosan and TBA modifier.

RESULTS AND DISSCUSION

The presence of specific reactive groups grafted to the chitosan chain was confirmed by ^{1}H NMR spectroscopy in the case of maleimide–functionalized chitosan. Figure S1 shows the ^{1}H NMR spectra of neat chitosan and CsMal. The characteristic proton signals of the glucosamine unit appeared in the range of 4.50–2.50 ppm (1–6)[1]. The peak close to 1.90 ppm was attributed to the proton signal of the methyl group of the acetamido moiety. The insertion of the maleimide ring into the polymer structure could be confirmed by the peak at 6.27 ppm (a) in the CsMal spectrum, which corresponds to the protons of the double bond of the ring –CH=CH–[1].

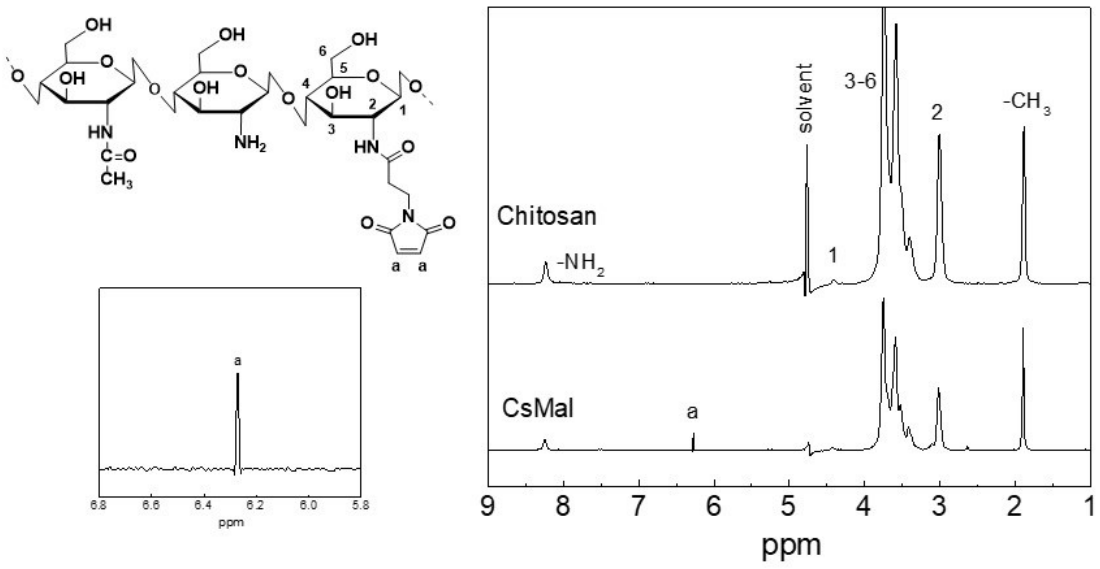

Figure S1. Liquid–state ^{1}H NMR spectra and chemical structure of chitosan and maleimide–functionalized chitosan (CsMal).

The extent of amine substitution (degree of substitution) was quantitatively determined by Equation S1 and was found to be 10 %.

On the other hand, the degree of substitution of CsTZ was confirmed by solid–state ^{13}C NMR spectroscopy (Figure S2). As it could be observed, specific signals corresponding to the reactive tetrazole group grafted to the chitosan backbone clearly manifested in the spectrum of the chitosan derivative. The ^{13}C NMR spectrum of chitosan is characterized by the presence of one signal corresponding to the anomeric carbon (C_1) at 104.5 ppm and a second signal containing multiple peaks in the 90–45 ppm region, associated to the rest of carbons of the deacetylated glucosamine unit ($C_{2–6}$). Finally, the signals of the carbons of carbonyl and methyl groups of the acetamido moiety appear at 172.9 and 23.0 ppm, respectively.[13–16] The incorporation of the tetrazole ring into the polymeric structure could be confirmed by the signals in the range between 166–156 ppm ($C_{e,i}$) and 136–107 ppm ($C_{g–h}$), which corresponded to the carbons of the grafted molecule.[12] Furthermore, as the grafting of the

tetrazole groups into the chitosan led to the formation of new amide groups, the signal located at 172.1 ppm corresponding to the carbonyl groups was transformed due to the functionalization. In the same way, the signal corresponding to the methyl groups at 24.3 ppm was notably transformed after the incorporation of the tetrazole molecules, since the amount of terminal $–CH_3$ groups on the CsTZ sample was also affected.

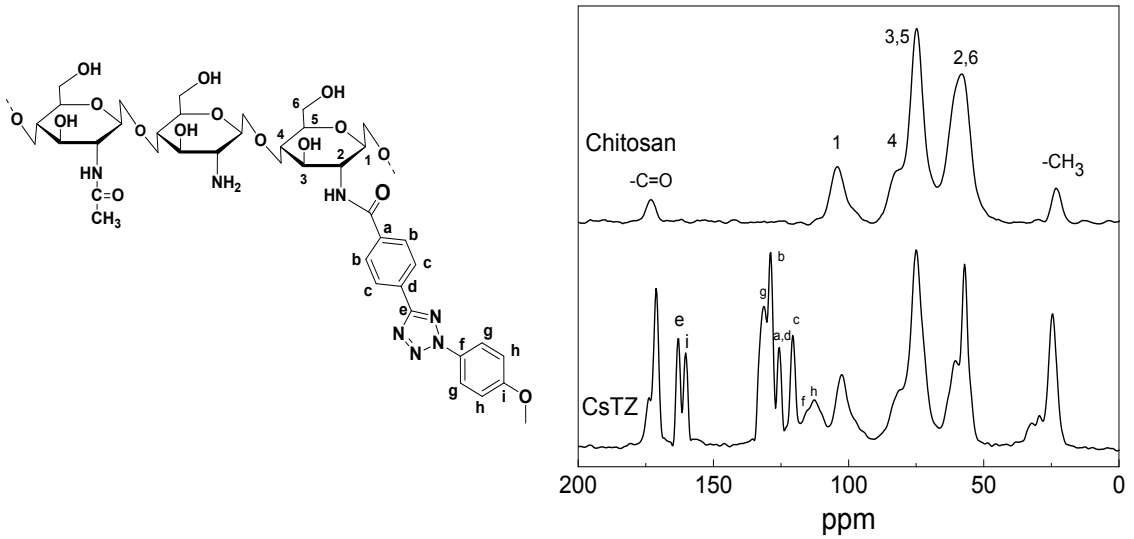

Figure S2. Solid–state ^{13}C NMR spectra and chemical structure of chitosan and tetrazole–functionalized chitosan (CsTZ).

The DS was determined by the integration of the areas of the carbon signals of the glucosamine units and those of the tetrazole unit that were not affected. Calculations were made using the Equation S2, where A_{TZ} corresponds to the area of tetrazole carbon signals in the range of 136–107 ppm and A_{Cs} to that of the glucosamine carbon units ($C_{3–5}$). The DS for the tetrazole–containing chitosan was 29 %.

The crystallinity of the neat chitosan and the modified samples was analysed by X–ray diffraction. XRD patterns are shown in Figure S3. Chitosan exhibits three characteristics peaks at 2θ about 10–10.5º, 16º and 20–20.5º. In

agreement with previous reports, the strongest peak at 2θ about 20º is assigned to crystal forms II from (110) planes, whereas the peak at 2θ about 10º corresponds to crystal forms I from (020) planes and the one at 2θ about 16º to the amorphous phase.[5,17,18] Moreover, the crystallinity index (CI^{XRD}) of CsMal and CsTZ was calculated using the Equation S3 and were found to be 0.18 and 0.39, respectively. As expected, after the functionalization process, the degree of crystallinity decreased.[19,20] Indeed, the peak at 2θ = 20º became broader and weaker, suggesting a higher amorphous form in the modified samples.[21]

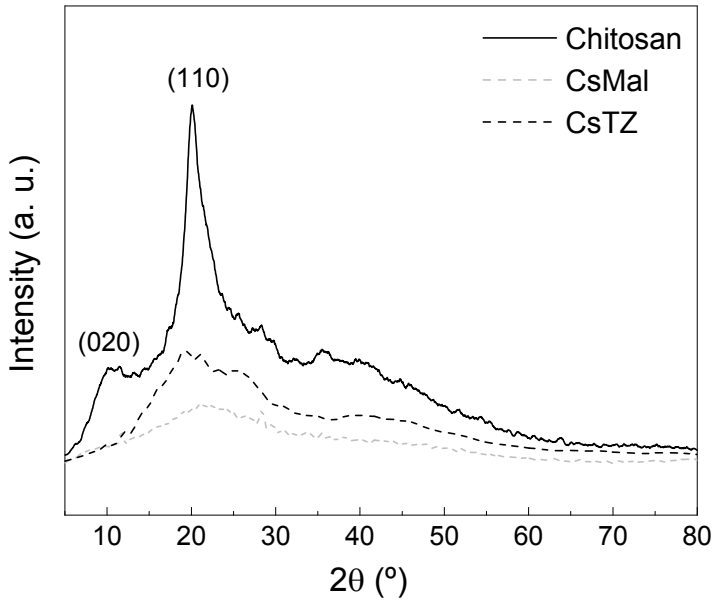

Figure S3. X–ray patterns of chitosan, CsMal and CsTZ.

The pore size distribution of freeze–dried CsTZ/CsMal hydrogels is shown in Figure S4.

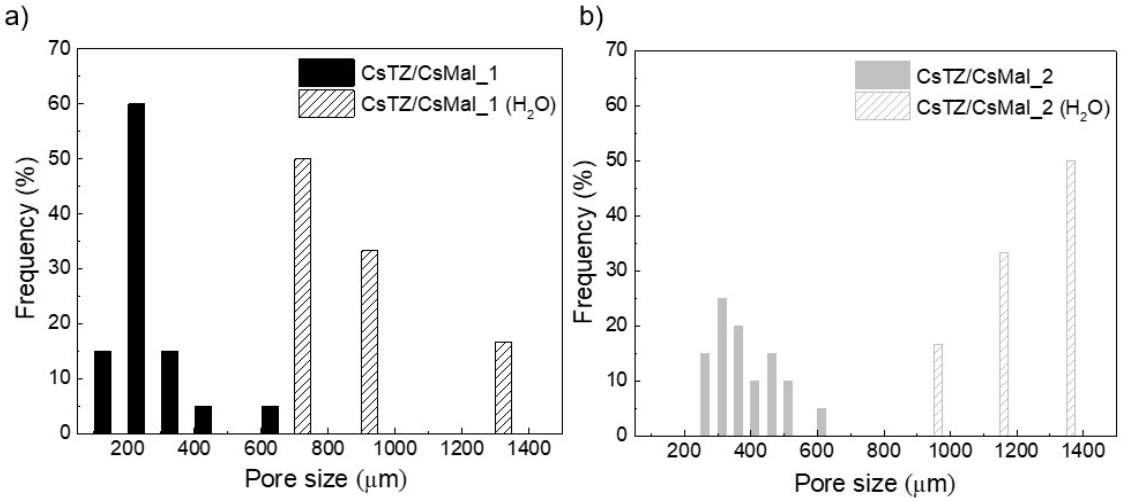

Figure S4. Pore size distribution for a) CsTZ/CsMal_1 and b) CsTZ/CsMal_2 hydrogels.

On the other hand, the addition of a higher amount of tetrazole–functionalized chitosan seemed to be contributing to the formation of a higher interconnected network, since lower swelling ratios were presented in both media. The swelling kinetics of the hydrogels was adjusted to Equation S11 and the obtained parameters (SR_{max}, k_S and r_o) are presented in Table S1, where SR_{eq} is the value of the swelling degree in equilibrium (48 hours). Greatly close values for SR_{eq} and SR_{max} in both media were obtained.

Table S1. Swelling parameters of CsTZ/CsMal hydrogels at 37 ºC in different aqueous media.

Swelling media	Hydrogel sample	SR_{eq} (%)	SR_{max} (%)	$k_S \cdot 10^4$ ($g_{hydrogel}$ $g_{solution}^{-1}$ s^{-1})	$r_o \cdot 10^3$ ($g_{solution}$ $g_{hydrogel}^{-1}$ s^{-1})
HCl	CsTZ/CsMal 1:50	778 ± 156	770	0.84	20
	CsTZ/CsMal 1:15	657 ± 90	640	0.21	116
PBS	CsTZ/CsMal 1:50	435 ± 21	440	0.50	103
	CsTZ/CsMal 1:15	354 ± 2	370	0.22	332

Regarding the pH, the absorption capacity of the hydrogels was higher in acidic medium. On the other hand, the lower swelling ratio values presented by the hydrogels in basic medium were related with higher r_o values as stated by Altinisik and Yurdakoc.[8]

REFERENCES

1 O. Guaresti, C. García–Astrain, T. Palomares, A. Alonso–Varona, A. Eceiza and N. Gabilondo, *Int. J. Biol. Macromol.*, , DOI:10.1016/j.ijbiomac.2017.04.003.

2 B. M. Chesnutt, A. M. Viano, Y. Yuan, Y. Yang, T. Guda, M. R. Appleford, J. L. Ong, W. O. Haggard and J. D. Bumgardner, *J. Biomed. Mater. Res. - Part A*, 2009, **88**, 491–502.

3 L. O. Ahmad, D. Permana, Wahab, S. H. Sabarwati, L. O. A. N. Ramadhan and U. Rianse, *Adv. Environ. Geol. Sci. Eng.*, 2015, 373–378.

4 Y. Yuan, B. M. Chesnutt, W. O. Haggard and J. D. Bumgardner, *Materials (Basel).*, 2011, **4**, 1399–1416.

5 A. V. Raut, R. K. Satvekar, S. S. Rohiwal, A. P. Tiwari, A. Gnanamani, S. Pushpavanam, S. G. Nanaware and S. H. Pawar, *Des. Monomers Polym.*, 2016, **19**, 445–455.

6 J. Karvinen, T. O. Ihalainen, M. T. Calejo, I. Jönkkäri and M. Kellomäki, *Mater. Sci. Eng. C*, 2019, **94**, 1056–1066.

7 F. Cyriac, P. M. Lugt and R. Bosman, *Tribol. Trans.*, 2015, **58**, 1021–1030.

8 A. Altinisik and K. Yurdakoc, *Polym. Bull.*, 2014, **71**, 759–774.

9 R. V. Badhe, D. Bijukumar, D. R. Chejara, M. Mabrouk, Y. E. Choonara, P. Kumar, L. C. du Toit, P. P. D. Kondiah and V. Pillay, *Carbohydr. Polym.*, 2017, **157**, 1215–1225.

10 M. Fan, Y. Ma, J. Mao, Z. Zhang and H. Tan, *Acta Biomater.*, 2015, **20**, 60–68.

11 S. Saravanan, A. Chawla, M. Vairamani, T. P. Sastry, K. S. Subramanian and N. Selvamurugan, *Int. J. Biol. Macromol.*, 2017, **104**, 1975–1985.

12 C. Rodriguez-Emmenegger, C. M. Preuss, B. Yameen, O. Pop-Georgievski, M. Bachmann, J. O. Mueller, M. Bruns, A. S. Goldmann, M. Bastmeyer and C. Barner-Kowollik, *Adv. Mater.*, 2013, **25**, 6123–6127.

13 C. Lefay, Y. Guillaneuf, G. Moreira, J. J. Thevarajah, P. Castignolles, F. Ziarelli, E. Bloch, M. Major, L. Charles, M. Gaborieau, D. Bertin and D. Gigmes, *Polym. Chem.*, 2013, **4**, 322–328.

14 C. Gartner, B. L. Löpez, L. Sierra, R. Graf, H. W. Spiess and M. Gaborieau, *Biomacromolecules*, 2011, **12**, 1380–1386.

15 I. Younes, S. Hajji, V. Frachet, M. Rinaudo, K. Jellouli and M. Nasri, *Int. J. Biol. Macromol.*, 2014, **69**, 489–498.

16 N. Liu, S. Ni, A. J. Ragauskas, X. Meng, N. Hao and Y. Fu, *J. Biotechnol.*,

2018, **269**, 8–15.

17 M. Jiang, K. Wang, J. F. Kennedy, J. Nie, Q. Yu and G. Ma, *Int. J. Biol. Macromol.*, 2010, **47**, 696–699.

18 M. Prabaharan and S. Gong, *Carbohydr. Polym.*, 2008, **73**, 117–125.

19 F. Feng, Y. Liu, B. Zhao and K. Hu, *Procedia Eng.*, 2012, **27**, 718–732.

20 S. Gokila, T. Gomathi, P. N. Sudha and S. Anil, *Int. J. Biol. Macromol.*, 2017, **104**, 1459–1468.

21 S. Kumar and J. Koh, *Int. J. Mol. Sci.*, 2012, **13**, 6103–6116.